Adsorption of brilliant cresyl blue using NaOH-activated biochar derived from sewage sludge

Majda Ben Ali[1*], *Yassmina* Bakhtaoui[2], *Majda* Flayou[3], *Mouatamid* El hazzat[1], *Aicha* Sifou[1], *Mohammed* dahhou[1], *Mohammed* Kacimi[1], *Abdellah* Benzaouak[4] and *Adnane* El Hamidi[1]

[1] Laboratory of Materials, Nanotechnologies and Environment, Faculty of Sciences, Mohammed V University in Rabat, Morocco

[2] Laboratory of Advanced Materials and Process Engineering, Department of Chemistry, Faculty of Sciences, Ibn Tofaïl University, B.P. 133, Kenitra 14000, Morocco

[3] Laboratory of Quality Control of Waters, National Office of Electricity and Drinking Water (ONEE), Rabat, Morocco

[4] Laboratory of Spectroscopy, Molecular Modeling, Materials, Nanomaterials, Water and Environment, Environmental Materials Team, ENSAM, Mohammed V University in Rabat, Morocco

Abstract. The treatment of sewage wastewater generates a substantial amount of sludge, which poses significant ecotoxicological and environmental challenges. Managing this sludge is critical, as traditional disposal methods carry risks: agricultural use can lead to environmental contamination, while landfill disposal raises concerns about solid waste management and the preservation of landfill sites. Our research focuses on converting this urban sludge into activated carbon. We employed various techniques to characterize NaOH-activated biochar, including infrared (IR) analysis. BET analysis revealed a specific surface area of 62.35 m^2/g. We also assessed NaOH-activated biochar for its effectiveness in adsorbing brilliant cresyl bleu (BCB). The SSE error calculations indicated a first-order adsorption, while the isotherms suggested a better fit with the Sips model, indicating heterogeneous adsorption with an ns value of 0.95. Our study highlights the effectiveness of biochar in adsorbing dyes such as brilliant cresyl bleu BCB.

Keywords: sewage sludge; Wastewater; Brilliant Cresyl Blue; Activated Biochar; Specific surface area

1. Introduction

Urban sludge, derived from wastewater treatment plants, poses a significant environmental challenge due to its content of various contaminants such as heavy metals, organic compounds, and pathogens [1]. Inadequate management can lead to soil and water pollution, odor nuisances, and health risks [2]. Among the proposed solutions, thermochemical conversion is particularly promising as it transforms sludge into valuable products [3]. The main thermochemical conversion techniques include pyrolysis [4], combustion [5],[6],[7], gasification [8], and hydrothermal carbonization (HTC) [9].

To improve the properties of biochar and convert it into activated carbon, chemical activation is necessary [10]. This process endows activated carbon with exceptional properties, such as high porosity and large specific surface area, essential for the adsorption of various contaminants [11]. Chemical activation can be performed using several agents, including KOH [12], H_3PO_4 [13], $ZnCl_2$ [14], and particularly NaOH [15]. The latter is highly effective in creating active sites on the carbon, thus enhancing its adsorption capacity. The activation process with NaOH typically involves mixing biochar with a NaOH solution [16]. This chemical activation promotes the formation of micropores and mesopores on the carbon, thereby increasing the specific surface area available for adsorption [17]. Activated carbons with NaOH are particularly effective in adsorbing textile dyes such as brilliant cresyl blue due to the creation of pores and their high specific surface area [18].

The adsorption mechanism relies on the interaction between the functional groups present on the surface of activated carbon and the dye molecules, allowing for the effective capture of these contaminants [19]. These properties make activated carbon a preferred material for industrial wastewater treatment. By adsorbing contaminants, it enables sustainable and efficient water purification while contributing to more sustainable management of sewage sludge [20]. Activated carbon is not only used for the adsorption of textile dyes but also for the removal of other organic and inorganic pollutants present in industrial effluents [21]. In this study, we applied chemical activation to enhance the specific surface area of biochar. To thoroughly assess the effects of this activation, we performed several analyses, including infrared spectroscopy (IR) and Brunauer-Emmett-Teller (BET) analysis. The primary goal was to carefully examine the adsorption efficiency by producing activated carbon from urban sludge.

* Corresponding authors: majda-benali@um5r.ac.ma

© The Authors, published by EDP Sciences. This is an open access article distributed under the terms of the Creative Commons Attribution License 4.0 (https://creativecommons.org/licenses/by/4.0/).

2. Materiels and methods

2.1 Materiels

The sewage sludge, collected from a municipal wastewater treatment plant in Ifrane, Morocco, was utilized to produce activated carbon. The procedure involved multiple stages. Initially, the sludge was dried in an oven at 100°C for 48 hours. Next, it underwent pyrolysis, where the dried sludge was carbonized in a programmable furnace with a heating rate of 5°C/min up to 500°C and maintained at this temperature for 1 hour. The resulting biochar was then subjected to chemical activation using KOH at a concentration of 1 mol with 4 g of biochar. Finally, the activated biochar was dried and neutralized.

2.2 Characterizations of the prepared activated carbon

To analyze the functional groups in urban sludge and NaOH-activated biochar, Fourier-transform infrared spectroscopy (FTIR) was performed in transmission mode using a Nicolet iS50 spectrometer, which spans the spectral range of 400 to 4000 cm^{-1}. The specific surface area (S_{BET}) of the biochar was determined through nitrogen adsorption experiments at 77 K, using a NOVA 2200 instrument (Quantachrome Corp.) and applying the Brunauer-Emmett-Teller (BET) equation.

2.3 Methods

2.3.1 Kinetics and equilibrium modeling

The kinetic data were analyzed using both Lagergren's pseudo-first-order (equation 1) and pseudo-second-order (equation 2) models [22]. For evaluating equilibrium data, the Freundlich (equation 4) [23], Langmuir (equation 3) [23], and Sips [24] (equation5) adsorption models were applied . The models and their corresponding equations are outlined below:

- Pseudo first-order kinetic model

$$Q_t = Q_e(1 - e^{-k_1 t}) \quad (1)$$

Q_e (mg. g^{-1}) represents the amount of adsorbate material adsorbed at equilibrium, while Q_t (mg. g^{-1}) indicates the quantity adsorbed at a specific time t. The rate constant k_1 (min^{-1}) is determined from the slope of the plot of ln (Q_e - Q_t) against time.

$$Q_t = \frac{k_2 Q_e^2 t}{1 + k_2 Q_e} \quad (2)$$

Here, k_2 (min^{-1}): rate constant.

- Langmuir

$$Q_e = \frac{Q_m K_L C_e}{1 + C_e K_L} \quad (3)$$

Q_e (mg. g^{-1}) signifies the quantity of adsorbate retained at equilibrium, reflecting the amount held by the adsorbent. C_e (mg L^{-1}) represents the equilibrium concentration, which is the level at which the adsorption process stabilizes. Q_m (mg. g^{-1}) denotes the maximum theoretical adsorption capacity, indicating the maximum number of adsorbate molecules that can be bound by the adsorbent. K_L (L. mg^{-1}), the Langmuir constant, is related to the free energy associated with the adsorption process.

- Freundlich

$$Q_e = K_f C_e^{\frac{1}{n}} \quad (4)$$

K_f is a constant associated with the adsorption capacity, while 1/n is an empirical parameter that reflects the surface affinity of the adsorbent.

- Sips

$$Q_e = \frac{Q_m (a_s C_e)^n}{1 + (a_s C_e)^n} \quad (5)$$

In this context, the constants Qm, as, and n represent the adsorption capacity of the system (mg/g), the adsorption affinity constant (L/mg), and the heterogeneity index of the system, respectively.

3. Results and discussion

3.1 Fourier Transform Infrared Spectroscopy (FTIR)

Figure 1 presents the FTIR spectra of raw urban sludge and NaOH-activated biochar, revealing distinct variations between the samples. Raw urban sludge shows peaks at 3445.74 cm^{-1} (OH groups), 2963.14, 2919.34, and 2,849.35 cm^{-1} (-CH), 1633.92 cm^{-1} (C=O), 1539.42 and 1465.67 cm^{-1} (amide I and II), 1399.60 cm^{-1} (C=C bond), 1244.36 cm^{-1} (C-O groups), and 1041.43 cm^{-1} (C=O groups), along with 529.37 cm^{-1} (Si-O vibrations) [25]. After pyrolysis and NaOH activation, the FTIR spectrum of biochar shows the disappearance of peaks at 2963.14, 2919.34, and 2,849.35, 1633.92, 1399.60, and 1244.36 cm^{-1}, and a reduction in the peaks at 1041.43 cm^{-1}. The peaks at 875.06, and 1,465.67 cm^{-1} remain unchanged. A new OH peak appears at 3320.82 cm^{-1} during NaOH activation.

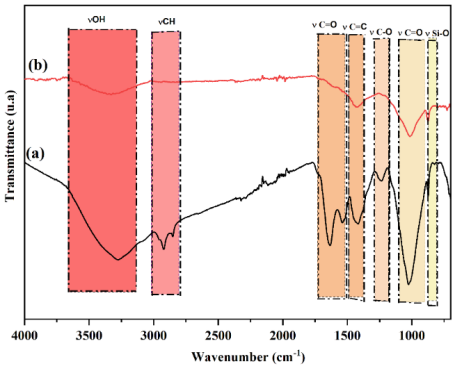

Fig. 1. FTIR spectra of (a) dried sewage sludge (b) biochar and (c) NaOH-activated biochar.

3.2 Surface area (BET)

The specific surface area (S_{BET}) of the samples is significantly different, indicating the impact of NaOH activation on biochar. The dried sewage sludge has a relatively low SBET of 5.295 m^2/g, suggesting limited porosity and surface area. In contrast, the NaOH-activated biochar shows a substantially higher SBET of 62.356 m^2/g, reflecting a much greater surface area and porosity. This increase in SBET demonstrates the effectiveness of NaOH activation in enhancing the adsorptive properties of biochar [26].

Table 1. Surface Area (S_{BET}) Comparison of Sewage Sludge and NaOH-Activated Biochar

	S_{BET} (m^2/g)
Sewage sludge	5.295
Activated biochar by NaOH	62.35

3.3 Adsorption experiments

3.3.1 Effects of Adsorption Parameters

This study explored the influence of various operational parameters, such as adsorbate concentration, adsorbent mass, pH, and the contact time between the adsorbate and the adsorbent, on the adsorption of BCB by KOH-activated biochar.

3.3.1.1 Mass effect

This research evaluated the effect of various operational parameters, including the adsorbate concentration, the amount of adsorbent, and the pH, on the adsorption of BCB by biochar activated with NaOH.

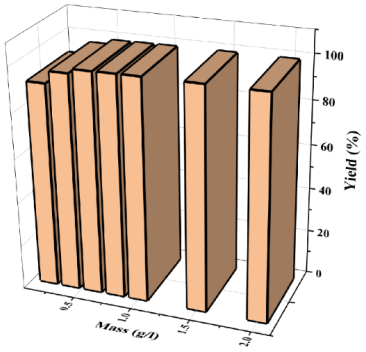

Fig. 2. The influence of the mass of NaOH-activated biochar on the 3D adsorption of Brilliant Cresyl Blue (BCB).

Figure 2 shows that as the mass of NaOH-activated biochar increases, the adsorption of Brilliant Cresyl Blue (BCB) dye also increases, leading to almost complete removal of the dye from the solution. The removal percentage improved from 91% to 99%. These findings indicate that even with lower masses, the activated biochar significantly removes the dye. The 3D representation demonstrates that beyond a mass of 0.6 g/L, additional amounts result in similar removal percentages. Consequently, 0.6 g/L was determined to be the optimal mass for maximizing dye removal [27].

3.3.1.2 Impact of pH on BCB Removal

To investigate the effect of pH on the adsorption of BCB by NaOH-activated biochar in 3D (Fig. 3), we examined how this parameter influences the removal of BCB dye and its impact on the solution. The pH levels were adjusted between 4 and 10 using hydrochloric acid (HCl, 0.1 M) and sodium hydroxide (NaOH, 0.1 M). The BCB concentration was set at 50 ppm, with a biochar mass of 0.6 g/L (Fig.) and a contact time of 3 hours.

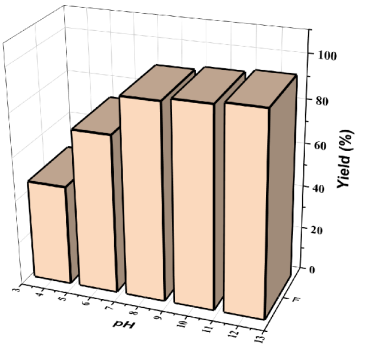

Fig. 3. Impact of pH on the adsorption of BCR by activated biochar by NaOH on 3D.

Figure 3 in 3D shows that the dye removal efficiency increases from 46% at pH 4 to 72% at pH 6, and further to 90% at pH 8. At lower pH levels, the surface can become positively charged, leading to competition between H^+ ions and dye cations, reducing the amount of dye adsorbed and thus the adsorption efficiency. At higher pH levels, the surface can become negatively charged, enhancing the adsorption of dye cations through electrostatic attraction, thereby increasing the adsorption of BCB. Consequently, maximum BCB adsorption at higher pH (basic conditions) involves equal amounts of anions and cations in the solution, which are neutralized and adsorbed onto the NaOH-activated biochar's adsorption sites [28].

3.3.2 Effect of contact time on BCB Adsorption

The effectiveness of NaOH-activated biochar was evaluated through the adsorption of BCB at room temperature (298 K), as shown in the 3D summary in Figure 4.

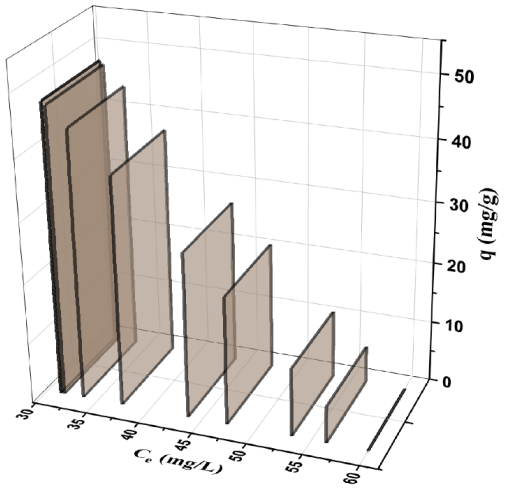

Fig. 4. The influence of contact time on the 3D adsorption of BCB using NaOH-activated biochar.

The results obtained revealed several significant observations (Fig. 4). During the first fifteen minutes, BCB removal by adsorption onto activated carbon experiences a rapid increase. This initial surge is primarily due to the high availability and easy accessibility of active sites on the activated carbon surface, facilitating the swift adsorption of BCB molecules early in the process. As time progresses, the rate of adsorption slows down because these active sites gradually become occupied. With fewer active sites remaining, the adsorption rate decelerates. After approximately 120 minutes, an equilibrium state is achieved, indicating that all active sites have been filled [29].

3.4 Adsorption kinetics modeling

The kinetic adsorption data reveal critical information about how adsorption reactions progress over time, which is vital for designing and modeling adsorption processes. To examine this, experimental data were compared against different kinetic models, such as pseudo-first-order and pseudo-second-order, as illustrated in Fig. 5. The fit between the experimental results and the model predictions was evaluated through nonlinear regression, using the sum of squared errors (SSE) as outlined in Table 2.

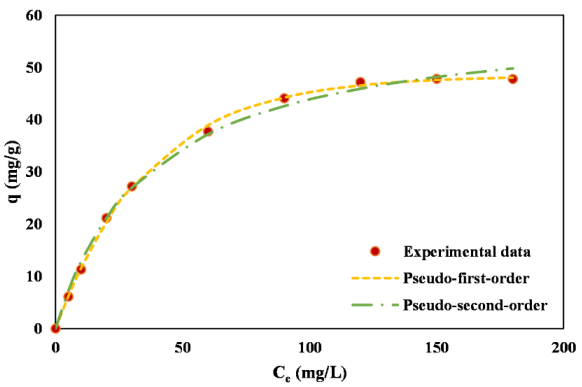

Fig. 5. Kinetic Models pseudo-first and pseudo-second order for Methylene Blue Adsorption onto Biochar KOH-Activated Biochar.

The kinetic analysis reveals significant variations in BCB adsorption capacities depending on the chosen model. The pseudo-second-order model forecasts an adsorption capacity (q_e) of 60.02 mg/g, while the pseudo-first-order model estimates it at 48.41 mg/g. Interestingly, the pseudo-first-order model offers a better fit to the experimental data, with a sum of squared errors (SSE) of 2.83, which is markedly lower than the 11.89 SSE observed with the pseudo-second-order model. Therefore, the pseudo-first-order model is more accurate in describing the adsorption kinetics of BCB on NaOH-activated biochar [30].

Table 2. Kinetic parameters for MB adsorption onto KOH activated biochar

Models	Parameters	Value
Pseudo-first-order	K_1 (min^{-1})	0.027

	$q_{e,exp}$	44.93
	$q_{e,th}$	48.41
	SSE	2.83
Pseudo-second-order	K_2 (min^{-1})	0.00045
	$q_{e,exp}$	47.86
	$q_{e,th}$	60.02
	SSE	11.89

3.5 Isotherm models

The interaction between methylene blue (MB) and activated biochar by KOH, and the adsorbate methylene blue was studied using several adsorption isotherm models, including Langmuir, Freundlich, Sips. To determine the most appropriate isotherm model, nonlinear regression was applied using the sum of squared errors (SSE) function. The parameters obtained from these models provide valuable information on the adsorption mechanisms, surface properties, and specific affinities of the adsorbents. The results of this study are presented in Fig. 6 and Table 5.

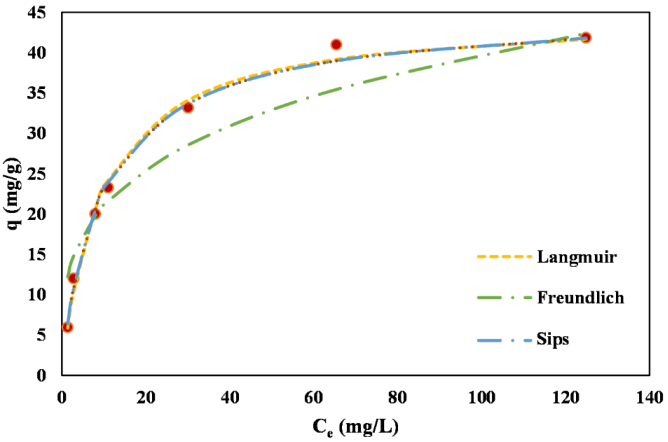

Fig. 6. Adsorption Isotherm Models for Methylene Blue onto Activated Biochar.

Figure 6 and Table 3 illustrate that the equilibrium data are best represented by the Sips isotherm model, as indicated by its favorable sum of squared errors (SSE) compared to the Langmuir and Freundlich models. The Sips model's normalized standard deviation (n_s) of 0.92 reveals a high degree of heterogeneity in the adsorption system, suggesting that BCB adsorption occurs on a surface with a range of adsorption sites, each with different energy levels. Thus, the results highlight that the adsorption of methylene blue occurs on a very heterogeneous surface, which is most accurately described by the Sips model [31].

Table 3. Isotherm parameters for the adsorption of methylene blue

Models	Parameters	Value
Langmuir	qm (mg. g^{-1})	44.81
	KL($L.mg^{-1}$)	0.11
	SSE	9.30
Freundlich	n	3.60
	KF (mg/g) $(mg/L)^{-}$ $^{1/n}$	11.10
	SSE	126.51
Sips	nS	0.92
	qm (mg. g^{-1})	45.88
	KS (L/mg)	0.12
	SEE	8.21

4. Conclusion

This study focused on improving the removal of textile dyes, with a particular emphasis on BCB. We investigated the creation of activated carbon from sewage sludge. Fourier-transform infrared spectroscopy (FTIR) revealed the formation of a distinct OH peak linked to the activating agent after chemical treatment. Additionally, BET analysis indicated a substantial increase in the specific surface area of the activated carbon, which rose to 84.68 m^2/g post-activation. We conducted a comprehensive assessment of KOH-activated biochar for its ability to adsorb BCB. The analysis of the sum of squared errors (SSE) suggests that the adsorption follows a first-order kinetics model, indicating precise kinetic behavior. Isotherm studies confirmed that the Sips model best represented the adsorption process, implying that the adsorption sites are heterogeneous. This research highlights the effectiveness of KOH-activated biochar for efficiently removing BCB from solutions.

References

1. K. Fijalkowski, A. Rorat, A. Grobelak, M. J. Kacprzak, Environ. Manage. **203**, 1126-1136 (2017)
2. A. Siddiqua, J. N. Hahladakis, W. A. K. A. Al-Attiya, Environ Sci Pollut Res. **29,** 58514-58536 (2022)
3. N. Gao, K. Kamran, C. Quan, P. T. Williams, Energy Combust. Sci. **79**, 100843, (2020)
4. M. W. Seo, S. H. Lee, H. Nam, D. Lee, D. Tokmurzin, S. Wang, Y. K. Park, Bioresour. Technol. **343** (2022)
5. M. Hu, Z. Ye, H. Zhang, B. Chen, Z. Pan, J. Wang, Environ. Pollut. Bioavailab. **33**, 145-163 (2021)
6. B. Rijo, C. Nobre, P. Brito, P. Ferreira, Energies. **17**, 2417 (2024)
7. Z. Kowalski, A. Makara, J. Kulczycka, A. Generowicz, P. Kwaśnicki, J. Ciuła, A. Gronba-Chyła, Energie. **17**, 1383 (2024)
8. N. Gao, K. Kamran, C. Quan, P. T. Williams, Prog. Energy Combust. Sci. **79**, 100843 (2020)
9. K. Czerwińska, M. Śliz, M. Wilk, Renew. Sustain. Energy Rev. **154**, 111873 (2022)
10. R. Kumar Mishra, B. Singh, B. Acharya, Carbon Resour. Convers. **7**, 100228 (2024)
11. X.-L. Zhu, P.-Y. Wang, C. Peng, J. Yang, X.-B. Yan, Chin. J. Chem. **25**, 929-932 (2014)
12. O. Oginni, K. Singh, G. Oporto, B. Dawson-Andoh, L. McDonald, E. Sabolsky, Bioresour. Technol. **7**, 100266 (2019)
13. R. Zakaria, N. A. Jamalluddin, et M. Z. Abu Bakar, Results Mater. **10**, 100183 (2021)
14. P. E. Hock, M. A. A. Zaini, Acta Chim. Slov. **11**, 99-106 (2018)
15. H. Shokry, M. Elkady, H. Hamad, J MATER RES TECHNOL. **8**, 4477-4488 (2019)
16. Y. Mu, H. Ma, Chem. Eng. Res. Des. **167**, 129-140 (2021)
17. R. L. Tseng, J. Colloid Interface Sci. **303**, 494-502 (2006)
18. V. S. Mane, P. V. V. Babu, Desalination. 273, 321-329 (2011)
19. S. Husien, R. M. El-taweel, A. I. Salim, I. S. Fahim, L. A. Said, A. G. Radwan, Curr. Res. Green Sustain. **5**, 100325 (2022)
20. N. M. Y. Al-mahbashi, N. A. Mutalib, A. O. Yagoub, I. F. M. Nor, A. Zainon Noor, S. M. Alhassan, J. Environ. Chem. Eng. **8**, 100437 (2023)
21. A. Bazan-Wozniak, R. Pietrzak, J. Chem. Eng. **393**, 124785 (2020)
22. S. Zafar, N. Khalid, M. Daud, M. L. Mirza, The Nucleus (2015).
23. N. Priyantha, L. B. L. Lim, M. K. Dahri, D. T. B. Tennakoon, J. Appl. Environ. Sci. **8**, 179-188 (2013)
24. I. Badran, R. Khalaf, Sep. Sci. Technol. **55**, 2433-2448 (2020)
25. M. Ben Ali, M. el Hazzat, M. Kacimi, M. Dahhou, A. Benzaouak, A. El Hamidi, NanoWorld J. **9** (2023)
26. Y. Lee, J. Shin, J. Kwak, S. Kim, C. Son, K. H. Cho, K. Chon, Energies. **14**, 1297 (2021)
27. Q. Ge, P. Li, M. Liu, G.-m. Xiao, Z.-q. Xiao, J.-w. Mao, X.-k. Gai, Bioresour. bioprocess. **10**, 51 (2023)

28. M. A. Baghapour, B. Djahed, M. Ranjbar, J Health Sci Surveillance Sys. **1** (2013)

29. R. Sadki, M. Dalimi, N. Labjar, G. A. Benabdallah, S. E. Hajjaji, Mor. J. Chem. **11**, 594-612 (2023)

30. A. A. Babaei, S. N. Alavi, M. Akbarifar, K. Ahmadi, A. Ramazanpour Esfahani, B. Kakavandi, DESALIN WATER TREAT. **57**, 27199-27212 (2016)

31. C. M. Navarathna, J. E. Pennisson, N. B. Dewage, C. Reid, C. Dotse, M. E. Jazi, P. M. Rodrigo, X. Zhang, E. Farmer, C. Watson, D. O. Craig, A. Ramirez, M. Walker, S. Madduri, D. Mohan, T. E. Mlsna, Processe*s*. **11**, 111 (2022)